Mean Intracellular Water Molecule Lifetime: Another Useful Breast DCE-MRI Biomarker?

Wei Huang[1], Xin Li[1], Luminita A Tudorica[1], Karen Y Oh[1], Sunitha B Thakur[2], Elizabeth A Morris[2], Yiyi Chen[1], Nicole Roy[1], Mark D Kettler[1], Jason A Koutcher[2], and Charles S Springer[1]

[1]*Oregon Health & Science University, Portland, Oregon, United States,* [2]*Memorial Sloan Kettering Cancer Center, New York, New York, United States*

Introduction: The use of the Shutter-Speed Model (SSM) for DCE-MRI pharmacokinetic data analysis shows significantly improved diagnostic accuracy in breast cancer detection, compared to the Standard Model (SM) (1-3). This is accomplished because the underestimation of K^{trans} (plasma to interstitium contrast agent (CA) transfer rate constant) by the SM (relative to the SSM) is substantially greater for malignant than benign lesions. The SM assumes that the inter-compartmental water exchange kinetics are always effectively infinitely fast: all exchange MR systems remain in their fast-exchange-limit [FXL] conditions (4). The SSM admits these systems can transiently depart their FXL conditions during CA bolus passage through tissue – due to the greater CA extravasation (3,5).

In addition to the conventional K^{trans} and v_e (interstitial volume fraction) parameters, an SSM fitting of DCE time-course data can also return a third parameter, the mean intracellular water molecule lifetime, τ_i, which accounts for the transcytolemmal exchange effects. A recent yeast cell suspension study (6) shows that τ_i is *inversely* correlated with cell membrane ion ATPase kinetics, a measure of metabolism. In this study, the characteristics of the τ_i parameter for malignant and benign breast lesions are explored, as well as τ_i relationships with other DCE-MRI parameters.

Methods: 157 patients with 172 suspicious breast lesions [89 patients with 92 lesions at institution A (IA); 68 patients with 80 lesions at institution B (IB)] consented to research DCE-MRI studies prior to standard care biopsy procedures. The 92 lesions at IA were mammographically negative, but referred for biopsies following clinical MRI diagnoses. The 80 lesions at IB were referred for biopsies following positive mammography and/or ultrasound diagnoses. The research DCE-MRI acquisitions were performed using 1.5T GE (IA) and 3T Siemens (IB) instruments with the body transmit and 4- or 7-channel phased-array bilateral breast receive RF coils. A 3D spoiled gradient-recalled-echo (GRE) sequence was used to acquire unilateral sagittal 3 mm-thick DCE-MRI images for all 89 IA and 14 IB patients, covering the breast with the suspicious lesion(s). A GRE-based 3D TWIST sequence (7) was used to acquire bilateral axial 1.4 mm-thick DCE images from the other 54 IB patients. 10^o flip angle and a parallel imaging acceleration factor of two were used in both sequences, with 2.2-4.2 ms TE and 5.6-7.4 ms TR for the former, and 2.9 ms TE and 6.2 ms TR for the latter. The unilateral acquisitions had a range of temporal resolution from 13 to 41 s (median: 25 s). TWIST is a k-space undersampling and data sharing GRE sequence delivering bilateral high spatial resolution breast DCE-MRI at uniform 18 s temporal resolution. The DCE-MRI acquisition time was ~8 (IA) or ~10 (IB) min with gadolinium CA (Magnevist® at IA and Prohance® at IB) IV injection through an antecubital vein (0.1 mmol/kg at 2 mL/s) carried out following acquisition of one (IA) or two (IB) baseline image volumes. The lesion ROI and pixel-by-pixel (within ROI) DCE time-course data were subjected to both the SM and the FXR-a (fast-exchange-regime-allowed) version SSM pharmacokinetic analyses to extract K^{trans}, v_e, k_{ep} (= K^{trans}/v_e, unidirectional CA intravasation rate constant) and τ_i (SSM only) parameters, as previously described (1-3).

Receiver Operating Characteristic (ROC) curve analyses were conducted to assess the diagnostic accuracies of the DCE-MRI biomarkers, while Spearman's correlation analyses were performed to evaluate relationships between τ_i and other biomarkers.

Results: Biopsy pathology analyses revealed that 46 of the 172 lesions were malignant. The **Table** lists the mean±SD lesion ROI DCE-MRI biomarker values for the malignant and benign lesions, as well as the ROC area under the curve (AUC) values with unity indicating perfect diagnostic accuracy. For both SM and SSM analyses, the malignant lesion group has significantly ($P < 0.0001$) higher K^{trans} and k_{ep} values than the benign group, while the SSM-only τ_i biomarker is significantly ($P = 0.02$) smaller for the malignant group compared to the benign group. There is no statistically significant difference in SM or SSM v_e values between the two groups. Based on ROC AUC values, K^{trans} and k_{ep} obtained from either model are good diagnostic markers with the SSM parameters having higher diagnostic accuracies than their SM counterparts. The difference in ROC AUC between SSM and SM K^{trans} is statistically significant ($P = 0.0013$, nonparametric test). The v_e and τ_i parameters are poor diagnostic markers.

Table Breast lesion ROI DCE-MRI parameters and corresponding ROC AUC values

	K^{trans} (min^{-1})		v_e		k_{ep} (min^{-1})		τ_i (s)
	SM	SSM	SM	SSM	SM	SSM	SSM
M (N=46)	0.12±0.06	0.21±0.14	0.36±0.17	0.61±0.17	0.36±0.16	0.34±0.24	0.49±0.22
B (N=126)	0.050±0.029[a]	0.056±0.036[b]	0.41±0.22	0.64±0.18	0.14±0.08[c]	0.094±0.060[d]	0.60±0.39[e]
ROC AUC	0.89	0.93	0.38	0.43	0.91	0.94	0.44

Mean ± SD; M: malignant; B: benign; unpaired t test (M vs. B): a, p<0.0001; b, p<0.0001; c, p<0.0001; d, p<0.0001; e, p=0.02.

Fig. 1 shows significant inverse correlations between SM K^{trans} and τ_i for the entire lesion population (left panel) and the malignant lesions (right panel). Similar significant correlation ($R = -0.16$, $P < 0.04$) was also found between SSM K^{trans} and τ_i for the entire population. Larger K^{trans} values are associated with smaller τ_i values. This can also often be seen within lesions, as the displacement of hot spots in parametric K^{trans} and τ_i maps. **Fig. 2** shows these color maps overlaid on DCE-MRI images from a malignant (top) and a benign (bottom) lesion. In both tumors, areas with "hot" K^{trans} color generally have "cold" τ_i color, and *vice versa*.

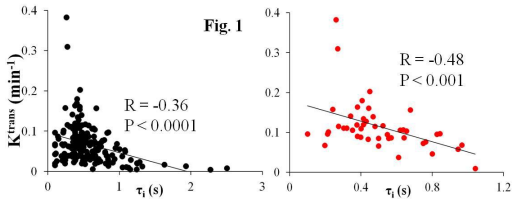

Discussion: Consistent with previous studies of smaller cohorts (1-3), substantial SM underestimation (relative to SSM) of K^{trans} occurred in only malignant lesions in this larger population. Since the FXL condition assumes $\tau_i \rightarrow 0$, the fact that malignant lesions have smaller τ_i values than benign lesions suggests that the greater increase of malignant lesion K^{trans} value by the SSM is not simply because it includes an additional variable (τ_i), but because of genuine exchange effects. The significant K^{trans}/τ_i correlation is not due to intra-model parameter co-variance because τ_i is a SSM-only parameter and it correlates with SM K^{trans}. τ_i has been shown to be inversely correlated with cellular metabolic activity (6). The smaller τ_i values for malignant lesions suggest that they are more metabolically active (as expected), but the τ_i hot spots areas within a malignant lesion may indicate regions of hypoxia/necrosis. This would be of tremendous clinical utility. K^{trans} has been shown to be a useful biomarker for prediction of breast cancer therapy response (8). The slope of the K^{trans}/τ_i linear regression is -0.13 for the malignant lesions (Fig. 1, right), indicating that a small, therapy-induced K^{trans} change may be reflected by a larger τ_i change. Thus, as potential measures of both tumor metabolism and perfusion/permeability, τ_i may be a very sensitive DCE-MRI biomarker for evaluation of breast cancer therapeutic response.

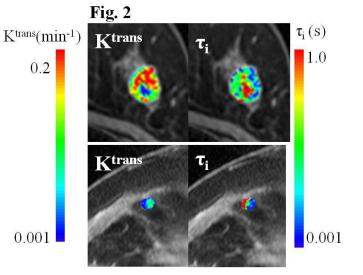

Grant Support: NIH: RO1-CA120861, UO1-CA154602, RO1-NS40801, RO1-EB00422.

References: **1.** Huang *et al. Radiology* **261**: 394-403 (2011). **2.** Springer *et al. Proc Intl Soc Magn Reson Med* **19**: 3097 (2011). **3.** Huang *et al. PNAS* **105**:17943-48 (2008). **4.** Tofts *et al. JMRI* **10**:223-32 (1999). **5.** Li *et al. PNAS* **105**:17937-42 (2008). **6.** Zhang *et al. Biophys J* **101**:000-000 (2011). **7.** Song *et al. Magn Reson Med* **61**:1242-8 (2009). **8.** Ah-See *et al. Clin Cancer Res* **14**: 6580-9 (2008).